Materiały Wysokoenergetyczne / High Energy Materials, **2022**, *14*: 58 − 75; DOI 10.22211/matwys/0224
ISSN 2083-0165

Research paper / Praca doświadczalna

Testing the attenuation capabilities of ballistic shields made using 3D printing
Badanie zdolności tłumiących osłon balistycznych wykonanych techniką druku 3D

Karolina Wierzbicka[1)], **Józef Paszula**[2,*)], **Roman Gieleta**[3)], **Zenon Komorek**[2)]

[1)] *Łukasiewicz Research Network – Institute of Aviation, Krakowska Ave. 110/114, 02-256 Warsaw, Poland*
[2)] *Military University of Technology, Faculty of Advanced Technologies and Chemistry, 2 gen. Kaliskiego St., 00-908 Warsaw, Poland*
[3)] *Military University of Technology, Faculty of Mechanical Engineering, 2 gen. Kaliskiego St., 00-908 Warsaw, Poland*
* *E-mail:* jozef.paszula@wat.edu.pl

ORCID Information:
Wierzbicka K.: 0000-0001-5850-7400
Paszula J.: 0000-0003-1908-6804
Gieleta R.: 0000-0003-2645-5321
Komorek Z.: 0000-0001-8103-3389

Abstract: *The paper describes a study of the blast wave energy absorption capabilities of sandwich ballistic shields. A comparative study of multilayer structures containing cores with different elementary cell shapes in their structure was performed. Energy-absorbing layers of different types of polymers were made. Tests of static and dynamic properties of the ballistic shield layers were carried out. The attenuation capabilities of these shields were determined by measuring the force acting on the base substrate of the shield.*

Streszczenie: *W pracy zaprojektowano i wykonano osłony balistyczne typu sandwich oraz przeprowadzono badania zdolności absorbowania energii fali podmuchowej. Przeprowadzono porównawcze badania struktur wielowarstwowych zawierających w swojej strukturze rdzenie o różnych kształtach komórek elementarnych. W badaniach przygotowano warstwy wykonane z różnych typów materiałów. Przeprowadzono badania właściwości statycznych i dynamicznych zaprojektowanych warstw osłon balistycznych. Zdolność tłumiącą wytypowanych osłon określano poprzez pomiar siły działającej na podstawę osłony.*

Keywords: *blast wave, blast wave attenuation, 3D printing technique, sandwich structures, negative Poisson's ratio, auxetic structures*

Słowa kluczowe: *fala podmuchowa, tłumienie fali podmuchowej, technika druku 3D, struktury typu sandwich, ujemny współczynnik Poissona, struktury auksetyczne*

1. Introduction

Terrorist attacks targeting civilian and government buildings, as well as areas with high population concentrations, have increased in intensity in recent years. Victims of attacks include people who have been affected by the direct impact of the shock wave, as well as structural damage to buildings [1]. Methods to reduce overpressure and blast wave pulse have been studied for many years and described in numerous publications. Systems including water baffles, air-filled microspheres, granular filters and geometric baffles, structures which change the direction of blast wave propagation, as well as foamed polymers and metals and sandwich-type multilayer structures, are considered [2-4]. Sandwich-type multilayer structures are characterised by their high strength and stiffness relative to weight [5], as well as their very good ability to absorb energy through plastic deformation. Once the yield point is reached, the deformation of the structures increases until the structure is completely compressed at constant stress [6]. They are typically used in aerospace, automotive as well as defence industries. The subject of the study consisted of multilayer structures made up of two outer layers (front and rear faceplate) and an inner core. The core had a cellular structure of different shapes [7]: vertical or diagonal walls, in the form of a lattice, a wave or inspired by nature. Figure 1 shows the diagram of a sandwich-type multilayer structure.

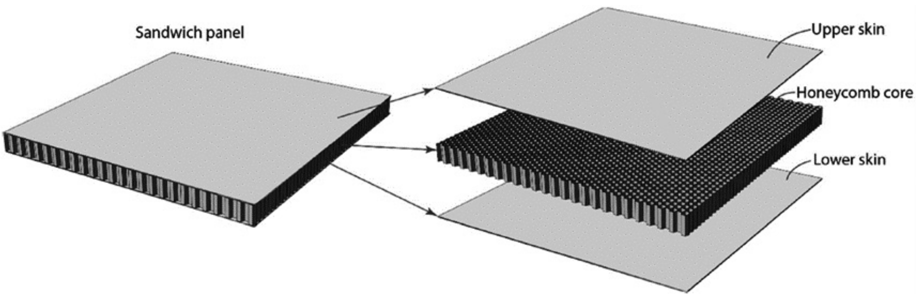

Figure 1. Schematic of sandwich layout design [8]

Materials with a negative Poisson's ratio (auxetic) have good energy absorption capacities and can thus make good protective structures. These systems are designed so that, under load, the thickening occurring in the internal direction is accompanied by an increase in strength [9].
This study attempts to test the feasibility of sandwich-type systems in ballistic shields, containing a cellular core made by 3D printing in ballistic shields. Structures made of three types of polymers with auxetic and non-auxetic cells were studied. The property tested was the structure's ability to absorb mechanical energy. Tests were carried out on samples of the structures in question using a comparative method based on the results obtained from static crushing tests and dynamic blast wave loading tests.

2. Characteristics of the materials used

2.1. Explosive

The explosive used during the tests was desensitized hexogen (6% wax addition), manufactured by Nitro-Chem S.A. In all systems, identical charges of pressed desensitized hexogen weighing 75 g, 30 mm in diameter and with a density of 1.67 g/cm^3.

2.2. Filaments

The models produced for the study were 3D printed using FFF (fused filament fabrication) technology. The polymers selected for the cellular structures were thermoplastic polyurethane (TPU), thermoplastic polyamide elastomer (PLA) and Nylon.

2.3. Structures selected for testing

Nine different core structures were designed for the study: 3 with a positive and 6 with a negative Poisson's ratio. The thickness of the cell walls was a constant value and was t = 0.8 mm. Other parameters were chosen so that the cells were of similar size. Figure 2 shows the designed structures with the elemental cells highlighted.

The AK (Figure 2, (5)) and AG (Figure 2, (9)) structures are larger in size due to the inability to print smaller or as a result of overlapping elemental cells. Some elemental cells, i.e. the smallest repeating structures throughout the core, are equivalent to a cell (the shape of the hole which forms the core) and some are part of it. The use of this approach stems from the need to adapt the shape of the elemental cell to the repeatability of the pattern in order to achieve the desired structure. The structures were assigned designations and the type of filament from which they were printed (Table 1). The first letter indicates the type of structure: N – non-auxetic, A – auxetic. The structures were printed from TPU, and the most popular (re-entrant honeycomb and honeycomb) additionally from PLA and nylon. Table 1 shows the designations of the tested structures with the assigned filaments.

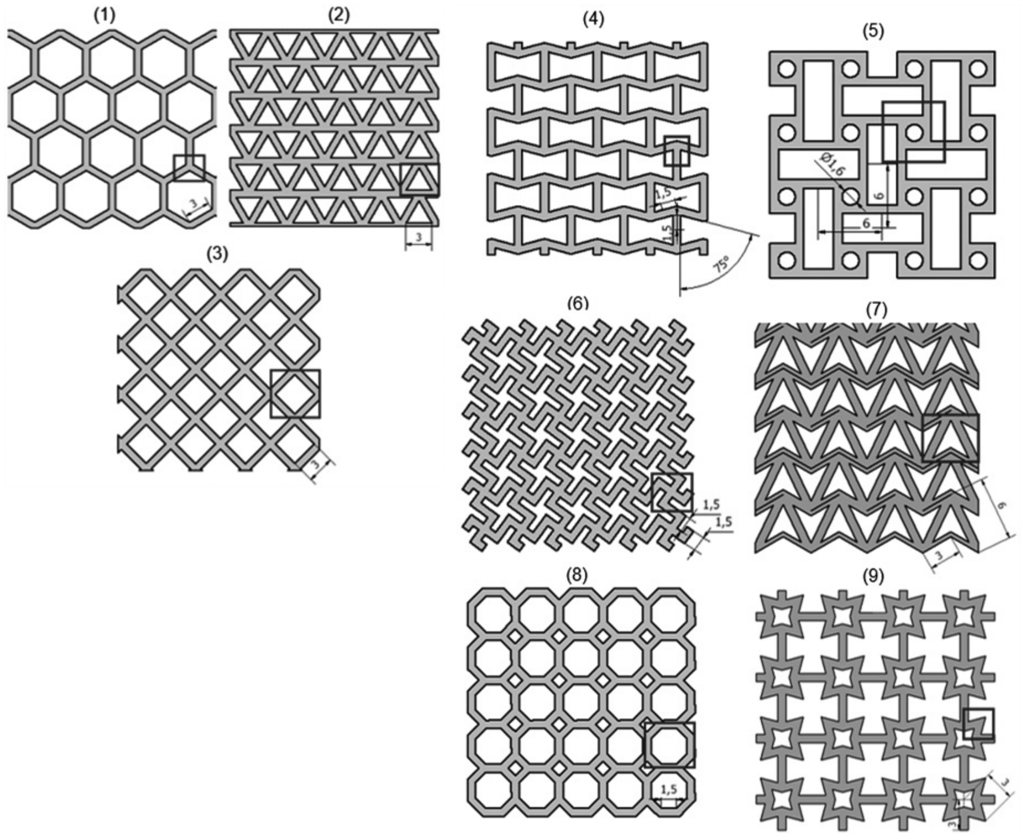

Figure 2. Non-auxetic structures: (1) – NHC, (2) – NHT, (3) – NHR, and auxetic structures: (4) – AHC, (5) – AK, (6) – ACB, (7) – AJ, (8) – ATB, (9) – AG

Table 1. Designation of structures with their associated filaments

Designation	Filament
AHC	TPU, Nylon (PA12), PLA
AK	TPU
ACB	TPU
AJ	TPU
ATB	TPU
AG	TPU
NHC	TPU, Nylon (PA12), PLA
NHT	TPU
NHR	TPU

2.4. Strength tests

2.4.1. Impact tests

In order to determine the behaviour of PLA, TPU and PA12 materials, impact tests were performed using a drop hammer. Figure 3 shows a schematic and photograph of the test bench.

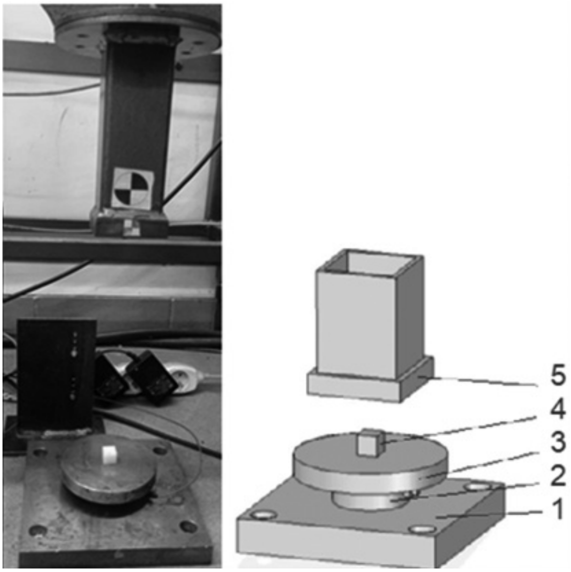

Figure 3. System for impact testing of cubes: 1 – steel base, 2 – transducers, 3 – anvil, 4 – sample, 5 – flat striker

A Piezotronics 200C50 PCB force transducer to 222 kN was used for the measurement. Striker displacement was measured using a Keyence LK-G502 non-contact laser transducer. The striker velocity was measured using two laser gates placed 50 mm apart. Signals from the transducer of force, displacement and laser gates were recorded using a computer and an NI USB-6361 analogue-digital measurement card from National Instruments, USA. Forces were recorded digitally with a sampling step of 10 ms. Station control and pre-processing of the measurement data were performed using a computer programme.
Tests were carried out on hexagonal solid cubes with a side length of 15 mm made of PLA, TPU and PA12. Tests were carried out at various impact velocities of a 15.3 kg hammer. Firstly, cubes made of PLA were examined. For an impact velocity of 2 m/s, the energy generated is destructive to a structure made of this

material. The samples were cracked, crumbled and crushed. Another material that tested was PA12 Nylon. For an impact energy corresponding to an impact velocity of 2 m/s, the specimens did not fail despite two attempts being made. However, for an impact velocity of 3 m/s, the impact energy was sufficient to destroy the sample material. TPU material samples were tested at energies corresponding to three impact velocities: 2, 3, 4 m/s. After the third test, the specimens did not deform, meaning that an impact velocity of 4 m/s does not cause permanent damage to the flexible TPU structure. The results of the measurements are shown in Figures 4-6.

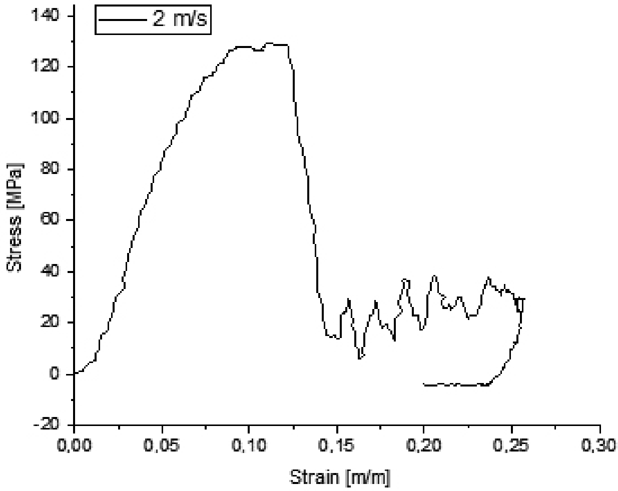

Figure 4. Deformation-stress curve of hexagonal cube made of PLA

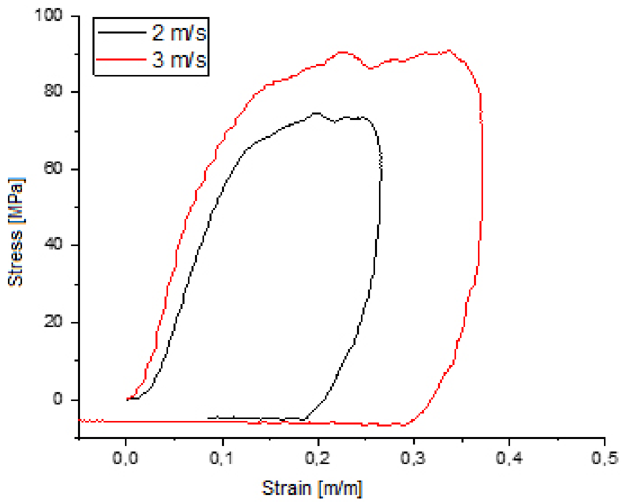

Figure 5. Deformation-stress curve of hexagonal cube made of PA12

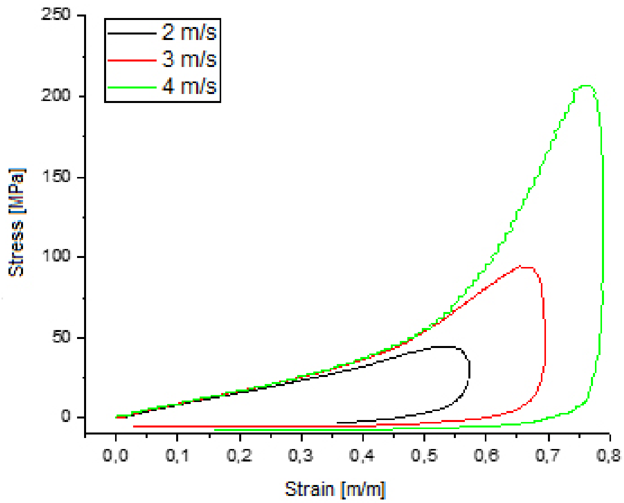

Figure 6. Deformation-stress curve of hexagonal cube made of TPU

All curves are characterised by an initial linear relationship, where the resulting stress is directly proportional to the deformation. This relationship is linear up to a certain stress limit and indicates elastic deformation of the material. The linear limit corresponds to the highest stress value beyond which the stress-deformation relationship is no longer linear. Once the elastic limit is exceeded, the material deforms plastically [11].
The elasticity coefficient was determined for PLA and PA12 materials. From the above curves, it can be seen that each material has a different deformation curve. PLA, being a brittle material, was damaged during the impact, becoming cracked and crushed, indicating that the highest stress occurred at the initial stage of the hammer impact, when the sample was not yet deformed. Nylon PA12 is a material with high resistance to stress cracking and is also slightly flexible. The maximum stress for this material for both hammer velocities occurred when the specimen was already in contact with the hammer. This stress was maintained at a similar level until the hammer rebounded. TPU is a very flexible, soft material which is susceptible to elastic deformation. For all velocity impacts, the profile of the curve is similar. The maximum stress in the material only occurs when the sample is crushed and the material is compressed. In rubber-like materials, deformation increases with increasing stress.
Table 2 shows the impact test results of the selected plastics. As the impact velocity and thus the kinetic energy increases, so does the energy absorbed by the material. TPU is able to absorb the greatest amount of energy before it plastically deforms.
The curves of impact test runs were analysed and the maximum stress (σ_m), the elasticity coefficient (as the directional coefficient of the rectilinear initial curve of the characteristic σ-ε), were determined. In addition, the work done to deform the tested materials in relation to the unit volume, was determined:

$$A = \frac{1}{V}\int_0^{\varepsilon_g} \sigma d\varepsilon \qquad (1)$$

where: A – work done to deform the material tested, V – volume of the sample tested, ε_g – limiting deformation corresponding to the maximum stress.

Table 2. Impact test results for PLA, PA12 and TPU

Material	Impact velocity [m/s]	Energy [MJ]	Maximum stress [MPa]	Coefficient of elasticity [MPa]
PLA	2	14.6	129	1834
PA12	2	13.7	74	764
	3	26.5	91	801
TPU	2	13.2	44	–
	3	26.4	94	–
	4	48.7	206	–

2.4.2. Static strength tests

In order to select the structures with the most promising damping capacities, static compression tests were carried out on an Instron 8501 testing machine. The actuating element of the machine is a hydraulic cylinder. The measuring range of the machine is a load of up to 100 kN using two force measurement sensors (10 kN and 100 kN), the displacement during testing is 100 mm. Static tests were performed using testExpert III software from Zwick Roell.
The tests were carried out in accordance with an in-house methodology, which is closest to the PN-EN ISO 604:2006 standard. Figure 7 shows a diagram of the dimensional determinations used in the calculations of the test specimens. All samples had similar dimensions as shown in Table 3. The table also shows the cross-sectional area values (S_0) of the samples (Equation 2). The differences in dimensions result from the need to print the entire cells of the structure.

$$S_0 = a \cdot b \quad (2)$$

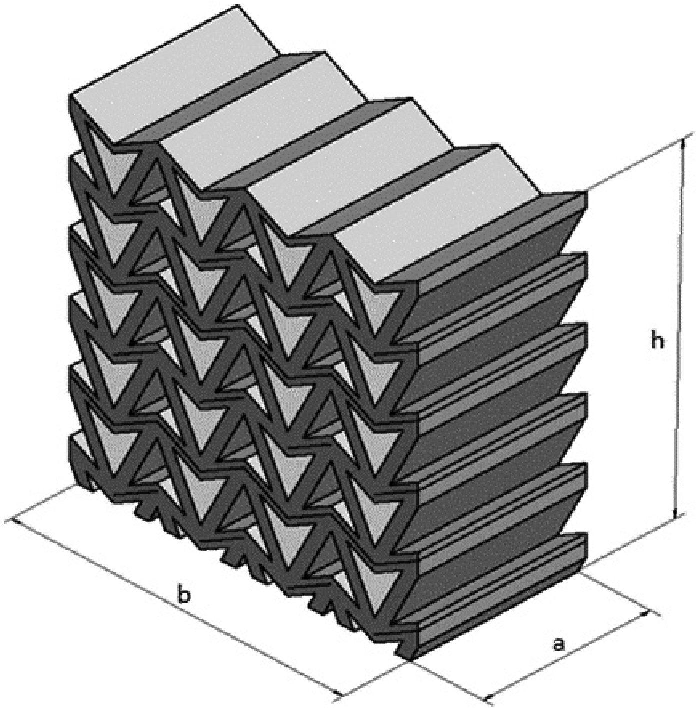

Figure 7. Dimensions of static test specimens

Table 3. Dimensions of static test specimens

Designation	*a* [mm]	*b* [mm]	*h* [mm]	S_0 [mm^2]
AHC (TPU)	9.8	22	20.6	215.6
AHC (PLA)	9.7	22.3	21.4	216.3
AHC (PA12)	10	22.5	21.5	225
ACB	9.8	22	22	215.6
AG	9.7	23	23	223.1
AJ	9.9	20.5	21.3	203
ATA	9.7	24.4	24.6	236.7
ATB	9.7	22.5	22.9	218.3
AK	9.8	21	20.5	205.8
NHC (TPU)	9.8	24	22.4	235.2
NHC (PLA)	9.7	24.7	22.9	239.6
NHC (PA12)	10	23.2	25	232
NHT	10	24.5	22	245
NHR	9.8	20.7	21.3	202.9

Auxetic structures become more compressed. The greatest thickening of the structure under applied force can be observed for the following: AHC, AJ and NHT. The high density of the NHT structure is due to the rigidity of its cells. Medium density of structures is observed for AG, AK, ATB and NHR, while low density is observed for NHC. Figure 8 shows the behaviour of the specimens under static loading.

On the basis of preliminary tests, it was assumed that, due to the non-linearity of the deformation above 80%, the limit range for conducting tests would not exceed 80% crushing. In addition, the deformation process of the samples would be carried out at a velocity of 4 mm/s. AHC and NHC structures made of TPU, PLA and Nylon PA12 were investigated. Figures 9-11 show the results of the static strength tests.

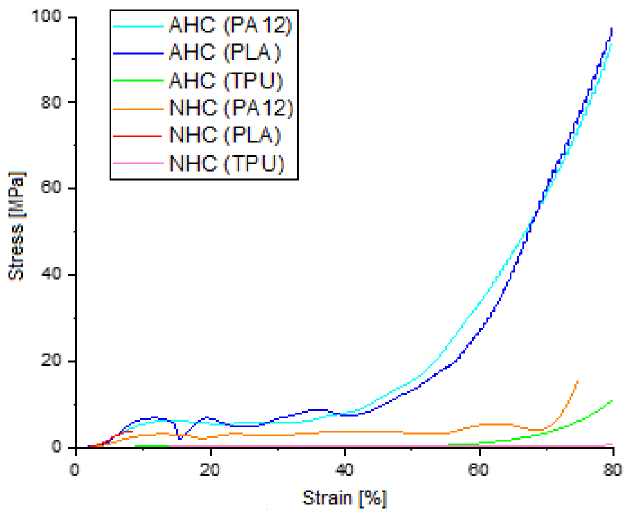

Figure 9. Relationship *f*(*ε*) = *σ* for specimens made from polymeric materials such as TPU, PLA and Nylon

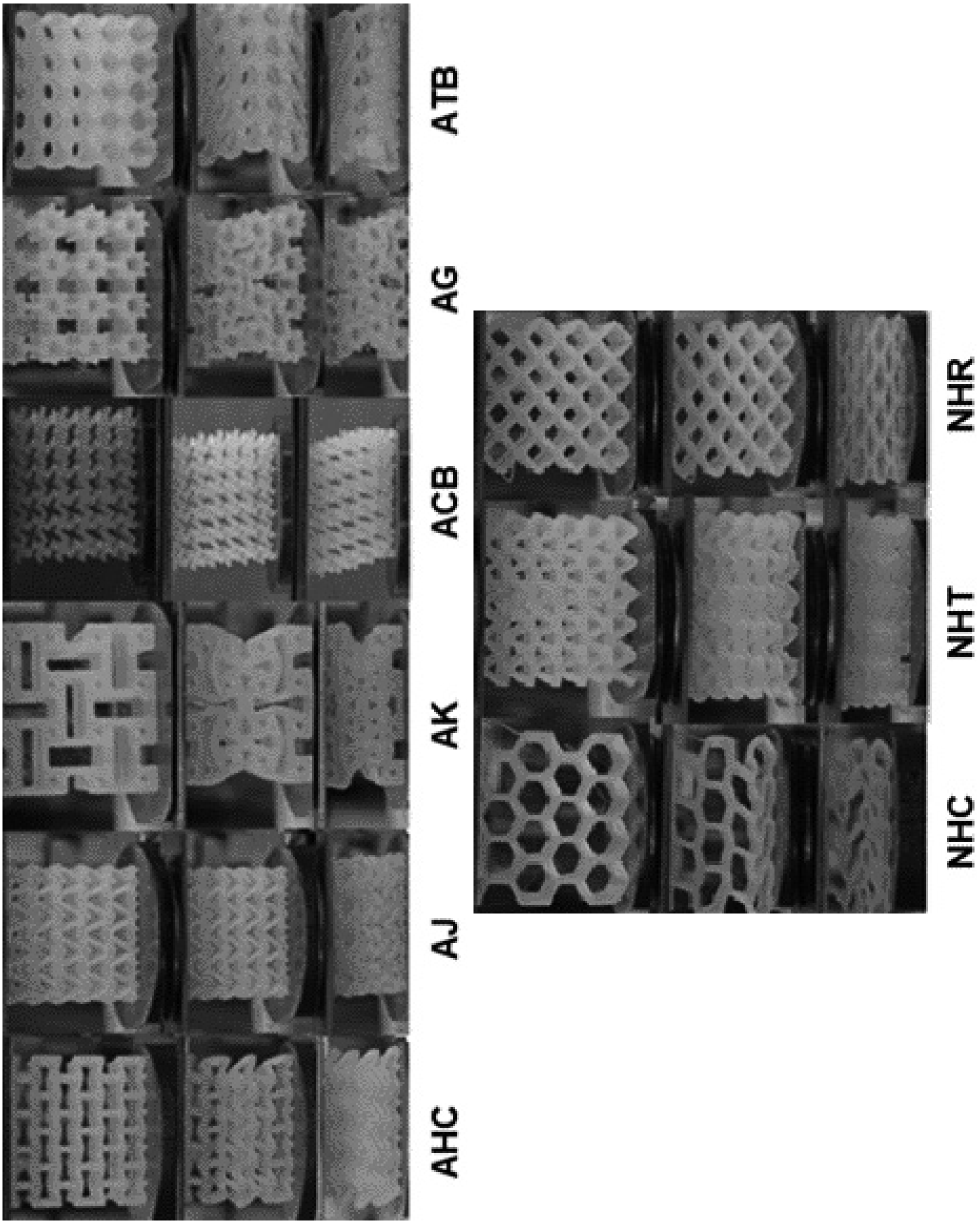

Figure 8. Behaviour of sample structures under static loading

It was clear from the study that the structure of the thermoplastic polylactide (PLA) exhibited brittleness and would not therefore, be the subject of further experiments. The polylactide polymer proved too brittle; cracking when force was applied. Structures made of TPU with negative and positive Poisson's ratio were investigated.

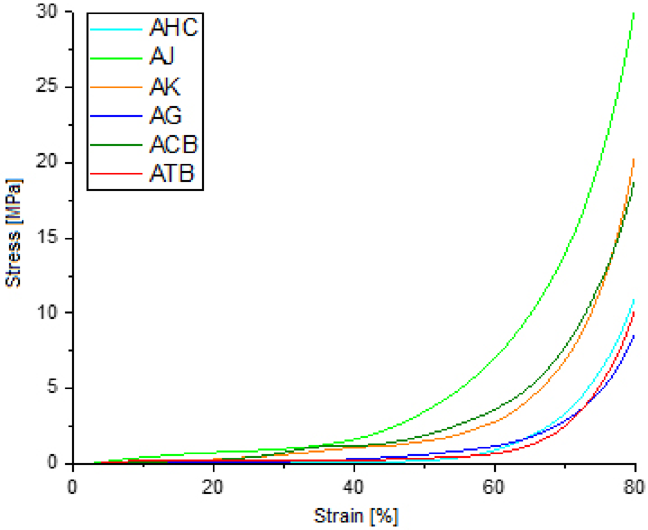

Figure 10. Relationship $f(\varepsilon) = \sigma$ for auxetic samples with

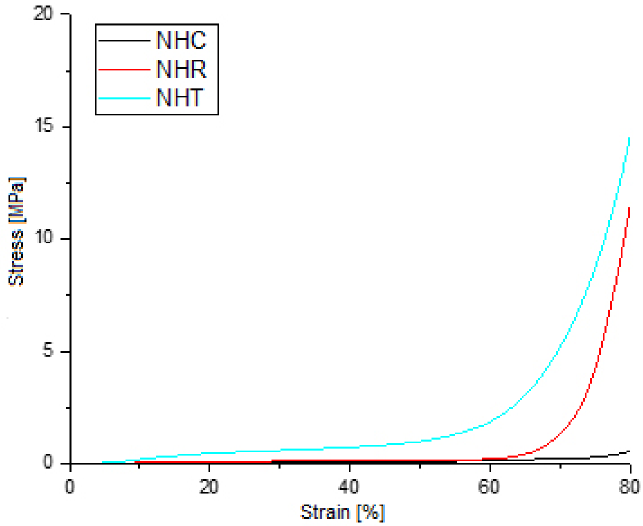

Figure 11. Relationship $f(\varepsilon) = \sigma$ for non-auxetic samples with TPU

From the resulting curves, the consolidation factor a, the energy without consolidation E_b and with consolidation E_u, the stress σ and the deformation e were determined for the selected energy (Figure 12).

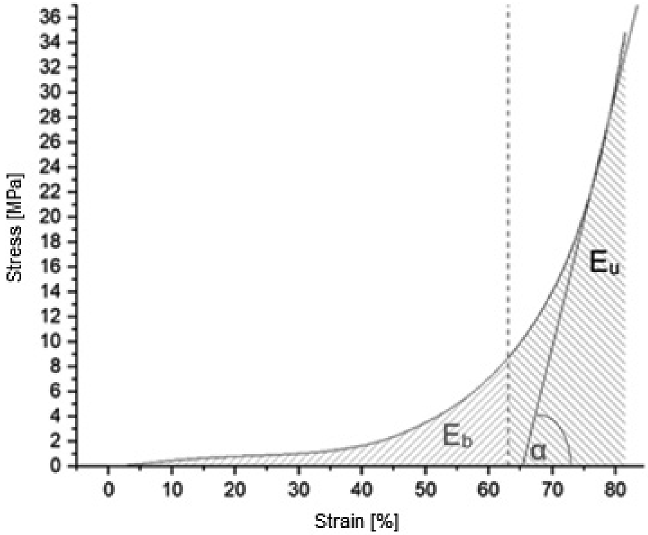

Figure 12. Diagram with the characteristic parameters of the structures highlighted

The consolidation factor, *a*, was determined by linearly approximating curves from 75-80% deformation. The non-consolidated energy E_b was determined by integrating the region from 0% to the deformation value for which the directional coefficient of the tangent to the deformation curve is tg30°, while the consolidated energy E_u was determined by integrating the region from this deformation value to 80%. The results are shown in Table 4.

Table 4. Values of consolidation factor and energy with and without consolidation

Designation	*a*	tg*a*	*e* for tg30° [%]	E_b [MJ]	E_u [MJ]
AJ	64	2.0469	63	1.3	2.9
ACB	54.5	1.4042	68	1	1.4
AG	38.3	0.7892	76	0.6	0.3
AK	61.3	1.8266	69	0.9	1.3
ATB	45.5	1.0176	73	0.4	0.5
AHC (TPU)	44.7	0.9899	46	0.4	0.5
AHC (PA12)	75.9	3.9917	63	6.6	11
AHC (PLA)	76.2	4.0557	48	2.8	14.2
NHR	49.4	1.1672	73	0.2	0.4
NHT	55.5	1.4566	71	0.8	0.9
NHC (TPU)	3	0.0519	Throughout the range, the slope of the curve does not reach tg30°		
NHC (PA12)	Deformation does not reach 75%		70	2.2	0.4
NHC (PLA)	The sample ruptured at the initial stage of testing				

The non-consolidation energy values obtained for structures made of PA12 and PLA are greater than 2 MJ. AHC (PA12) and NHC (PA12) also have the highest values for consolidation factors. Structures made from TPU are characterised by non-consolidation energy values in the range 0.2-1.3 MJ. The AJ, ACB and AK structures have the highest energies. The increase in E_b energy is associated with an increase in the consolidation factor.

3. Damping capacity of the tested absorber structures

3.1. Experimental setup

The testing of blast wave attenuation capacity was carried out on absorbers with the following structure: AJ, AK and ACB made of TPU, and NHC and AHC made of PA12 nylon. The tested absorbers were 95 mm in diameter and approximately 25 mm high. Figure 13 shows an example of the structure and the actual printed structure. Steel plates were glued to the finished prints: a 95 mm diameter and 2 mm thick upper plate and a 105 mm diameter and 3 mm thick lower plate.

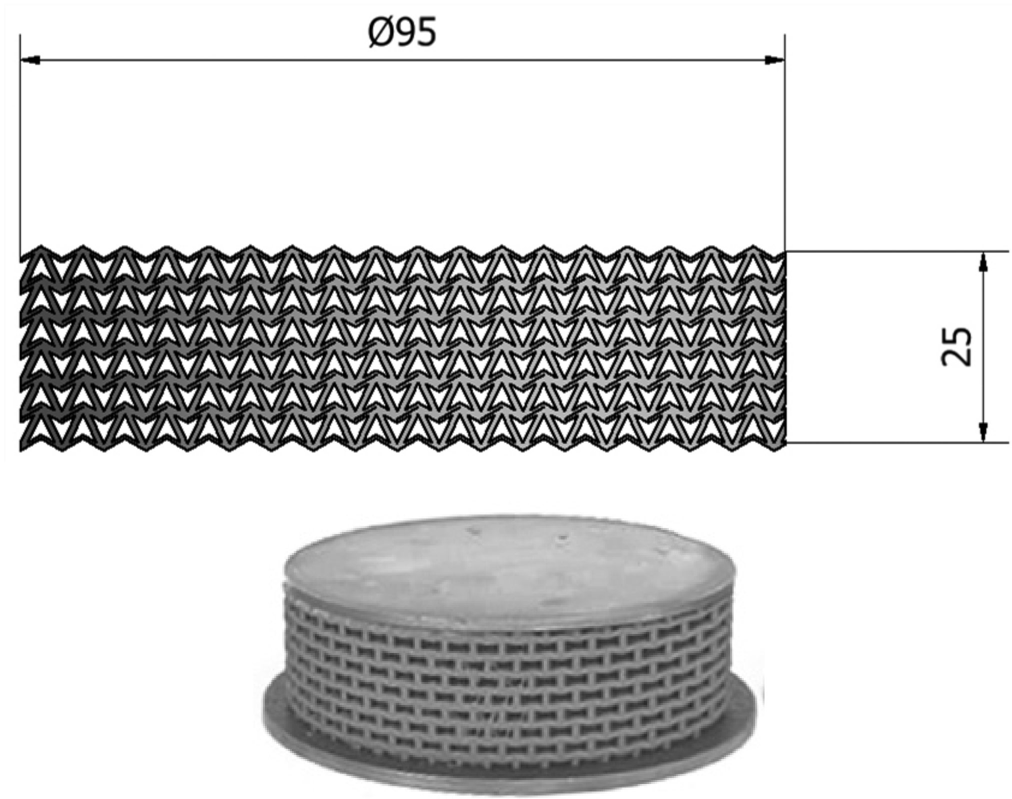

Figure 13. Blast wave absorbers

The test setup consisted of a test table on which sandwich-type structures were placed, a tube representing the distance between the lower absorber plate and the bottom of the explosive, and a 75 g RDX charge. A schematic of the setup and photographs are shown in Figure 14.

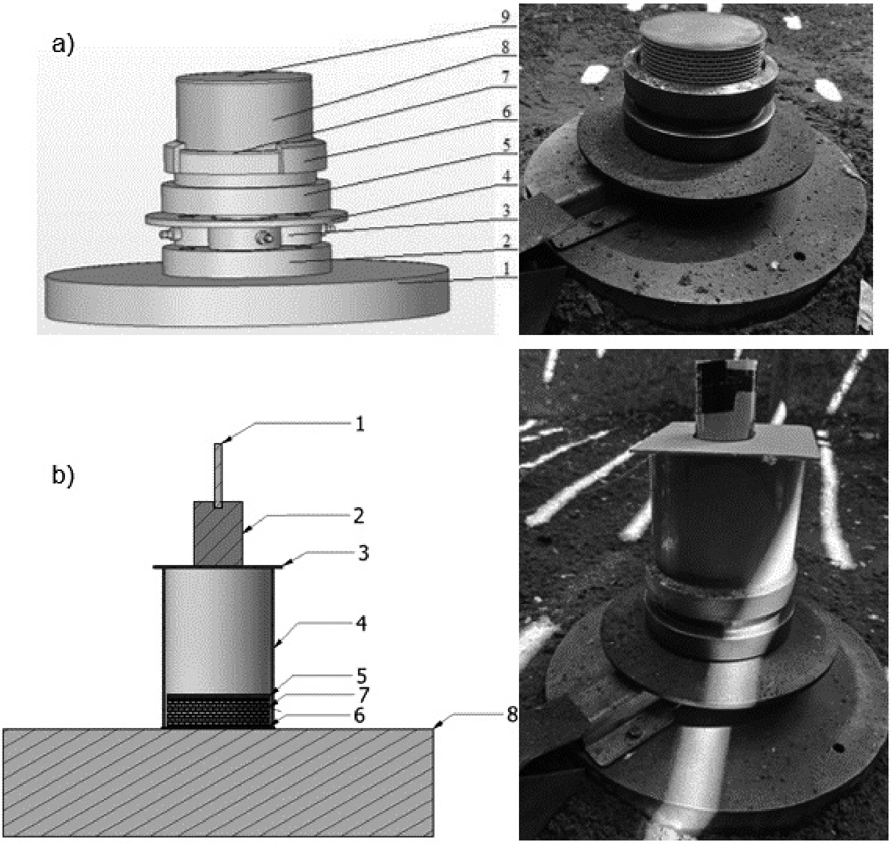

Figure 14. Test set-up for:
a) Measuring table for testing the energy consumption of printed sandwich structures : 1 – stand base, 2 – force sensor mounting plate, 3 – force sensors, 4 – protective plate, 5 – pressure plate, 6 – nut, 7 – force sensor mounting plate, (bottom faceplate), 8 – sample (core), 9 – top faceplate
b) System for testing absorption capacity by sandwich structures: 1 – detonator, 2 – explosive, 3 – cardboard pad, 4 – spacer, 5 and 6 – steel faceplates, 7 – core, 8 – table

Investigations into the energy consumption of printed structures during the impact of a blast wave were carried out using a table to measure the forces acting on the structure under test. A transducer mounting plate was placed on the base of the stand. Three Piezotronics model 200C50 PCB transducers rated to 222 kN, were used for the measurements. The pressure plate was attached to the base of the stand by three screws, which simultaneously exerted a slight initial pressure on the sensors. The test specimens were attached to the pressure plate using a nut and specimen fixing plate (front bottom plate). The blast wave load was transferred to the specimen using a steel plate with a diameter of 100 mm and a thickness of 3 mm. The transmitted force was measured using gauges to determine the ability of the 3-D fabricated structure under test to absorb it. The signals were recorded using a computer and an NI USB-6366 analogue-digital measurement card from National Instruments (USA). In the measurement system, the signals were digitally recorded with a sampling step of 0.5 μs on each channel. Pre-processing of the measurement data was done using a computer programme.

3.2. Test results

Before testing the damping capacity of the sandwich systems, the force recorded by the sensor was measured in the absence of the core (of structures selected for testing). For this purpose, two steel faceplates were glued together. Following the reference test, testing of the systems with the core proceeded. Systems with a core made of PA12 nylon with an auxetic (re-entrant honeycomb) and non-auxetic (honeycomb) structure were investigated. Figure 15 shows the curve of the force transmitted by the system under test.

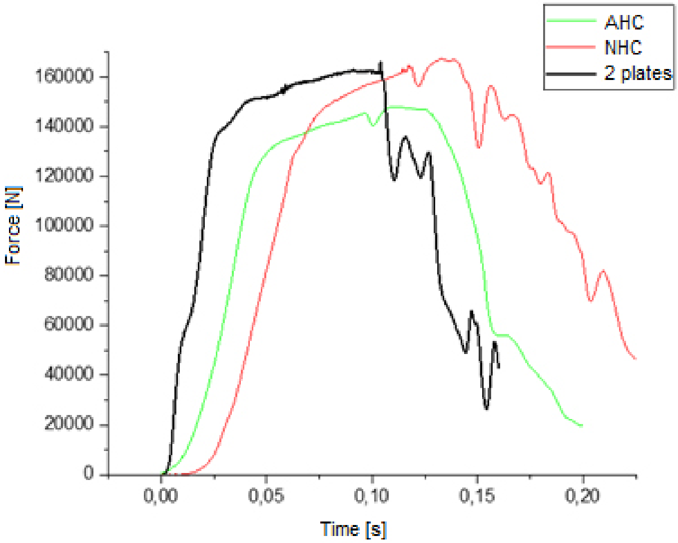

Figure 15. Force-time relationship for AHC and NHC structures

From the graph, it can be seen that the auxetic re-entrant honeycomb (AHC) structure absorbed more energy than the non-auxetic honeycomb (NHC) structure. In addition, AHC, unlike NHC, had not fragmented, but had been crushed.

The next study was carried out using structures with an auxetic core made of TPU. Figure 16 shows the structures before and after the tests. All TPU structures tested cracked where the printed core had defects. Defects which may have arisen include allowance or loss of material in the printed structure, displacement of the layer relative to the previous one, increased porosity or burning of the material, and filling of the material with impurities. Figure 17 shows the time characteristics of the force transmitted by the remaining absorbing structures.

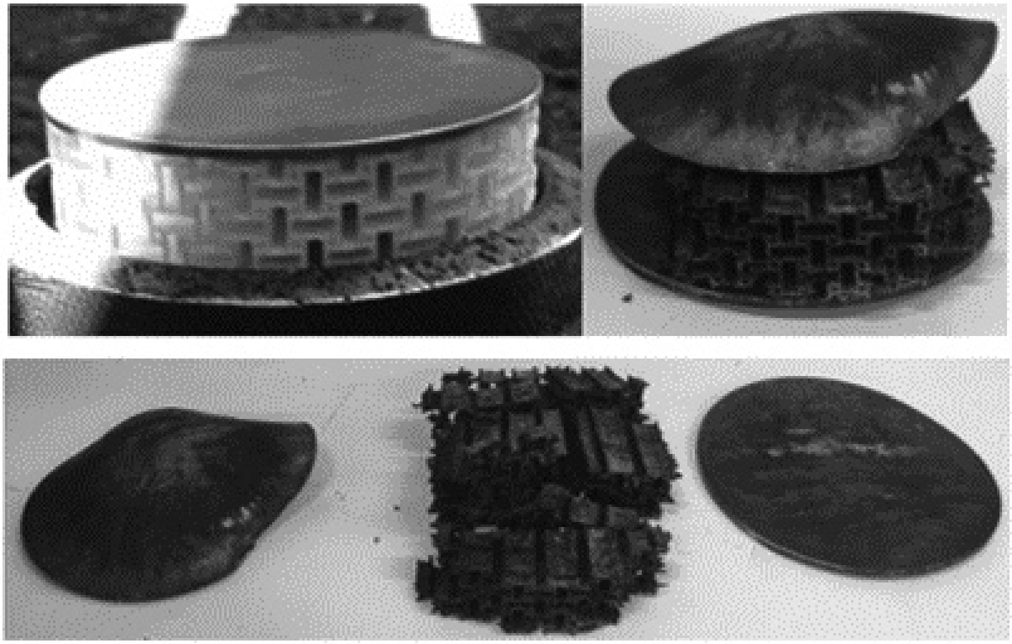

Figure 16. AK structure before and after the test

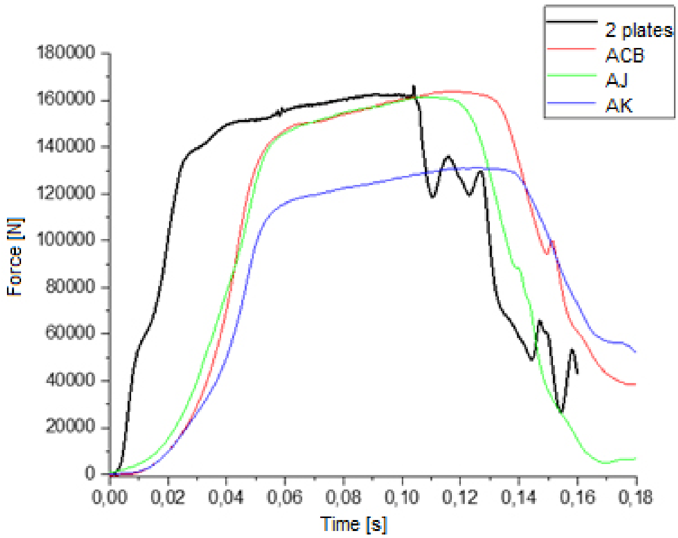

Figure 17. Force-time relationship for AJ, ACB and AK structure

From the graph, it can be seen that the AK structure absorbed the most energy. It had also undergone the greatest degree of fragmentation. For all curves, the maximum force F_m recorded by the table sensor was determined, the value I, which is proportional to the pulse, and the maximum pressure p_m, were determined. The I pulses of structures with a core were also compared with the pulse of a structure without a core I_0, and the p_m pressure of structures with a core with the p_{m0} pressure of a structure without a core. The results are shown in Table 5. The results corresponding to the reference test (2 plates) and the AK core system are shown in colour.

Table 5. Results of absorption capacity tests for sandwich structures

Designation	F_m [kN]	I [MPa×s]	p_m [MPa]	I/I_0	p_m/p_{m0}
2 plates	**166**	**0.52**	**5.87**	**1**	**1**
AHC	150	0.66	5.3	1.26	0.90
NHC	167	0.84	5.91	1.61	1.01
AK	**131**	**0.59**	**4.63**	**1.14**	**0.79**
AJ	161	0.58	5.7	1.11	0.97
ACB	164	0.64	5.8	1.23	0.99

Analysing the results obtained, it can be seen that, compared to the structure without a core (2 faceplates), the pulse value for each structure with a core increases. The largest increase in pressure values occurs for the non-auxetic NHC structure made of nylon, while the smallest increase occurs for the auxetic AK and AJ structures made of TPU. The smallest pulse value suggests that the momentum of the shielded body will be smallest after passing through the core structure. However, when comparing the overpressure value of structures with and without a core, it can be seen that it decreased for the auxetic structures, but increased slightly for the NHC structure. The lowest overpressure value was obtained for the AK structure. The force measured for the AK structure also had the lowest value. Figure 18 shows the pressure-pulse diagram for the systems studied. The layout without the core (2 plates) is shown in blue.

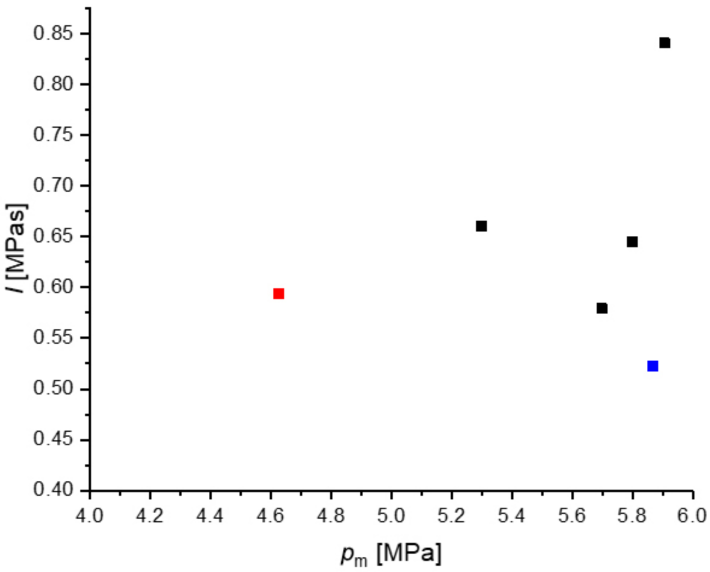

Figure 18. p_m-I diagram for sandwich structures

The coloured points correspond to the results highlighted in Table 5. Analysing the results of the measurements on the p_m-I plane, it can be seen that the AK structure (point highlighted in red) experienced a reduction in maximum pressure relative to the structure without the core, of approximately 20%. At the same time, a slight increase in pulse was observed for this case. This means that the AK structure has absorbed the most energy, so the overpressure-pulse pair after passing through the structure is the smallest.

4. Conclusions

- Analysis of the results from the impact tests showed that the spatial structure produced from PLA carries a high load but the material itself is brittle. This phenomenon was confirmed by the static crush tests. On the other hand, its biodegradability and rigidity are undoubted advantages. However, polylactide material is not a good material for making protective structures.
- Polyamide (nylon) PA12 on the other hand, is a very strong material with high resistance to cracking under load. Impact tests show that it is a less brittle material than PLA and more flexible. Strength tests during the static crushing test showed that structures made of PA12 absorb the highest (E_b = 6.6 MJ) amount of energy of the samples tested. This material absorbed more energy during the impact test than PLA before it deformed.
- Structures made of TPU polyurethane absorbed less energy (E_b = 0.4 MJ) than structures made of PA12. However, drop the drop-hammer tests showned that TPU is a polymer with high resistance to plastic deformation. This means that in order to permanently deform a structure made of polyurethane, a much higher load (>100 kN) must be applied, than to structures made of nylon.
  Based on the static strength tests, it was decided that the AJ, ACB and AK structures made of TPU would be tested for their blast wave damping capabilities. Two of the most popular AHC and NHC structures made of polyamide were also studied.
- Studies of structures with PA12 showed and confirmed the hypothesis that auxetic structures, due to their nature of deformation, are better energy absorbers than non-auxetic structures.
- Tests of TPU structures showed that the structure with the largest elemental cell (AK) dimensions is a better absorber than cells with smaller, more compact meshes. The AJ and ACB structures are rigid systems in which the blast wave is likely to have propagated through the walls of the structure. In the AK structure, on the other hand, the elemental cells were compressed (correct auxetic structure action). To crush such a structure, the blast wave did the most work and was therefore attenuated to the greatest extent.
- The measured and calculated results allow the following conclusions to be drawn:
  - The sandwich-type absorber structure with an AK cell-shaped auxetic core shows good blast wave attenuation capabilities.
  - TPU materials, due to the stretching of the polymer chains in their structure during deformation, are able to withstand high stresses before they are destroyed. They are therefore good materials for the cores of energy-absorbing sandwich systems.
  - Brittle polymers such as PLA or the slightly elastic PA12, despite their high absorption capacity and high loading strength, become crushed so that the core of the structure does not retain its properties and therefore show less damping capacity during dynamic loading than elastic materials.

References

[1] Shirbhate P.A., Goel M.D. A Critical Review of Blast Wave Parameters and Approaches for Blast Load Mitigation. *Arch. Comput. Methods Eng*. **2021**, *28*: 1713-1730.
[2] Wierzbicka K., Paszula J. Blast Wave Energy Absorbing Systems Made Using a 3D Printing Technique – Preliminary Research, *Mater. Wysokoenerg./High Energy Mater.* **2020**, *12*(2): 29-41.
[3] Langdon G.S., Nurick G.N., Balden V.H., Timmis R.B. Perforated Plates as Passive Mitigation Systems. *Def. Sci. J.* **2008**, *58*(2): 238-247.
[4] Komissarov P.V., Borisov A.A., Sokolov G.N., Lavrov V.V. Rigid Polyurethane Foam as an Efficient Material for Shock Wave Attenuation. *J. Phys. Conf. Ser.* **2016**, *751*: 012020.
[5] Jędral A. Rewiew of testing methods dedicated for sandwich structures with honeycomb core. *TAR*. **2019**, *2*(255): 7-20.

[6] Mullin M.J., O'Toole B.J. Simulation of Energy Absorbing Materials in Blast Loaded Structures. *Proc. 8th Int. LS-DYNA Users Conf.* Dearbon, MI, **2004**.
[7] Ha N.S., Lu G., Xiang X. Energy Absorption of a Bio-Inspired Honeycomb Sandwich Panel. *J. Mater. Sci.* **2019**, *54*: 6286-6300.
[8] Chen S., McGregor O.P.L., Endruweit A., Harper L.T., Warrior N.A. Simulation of the Forming Process for Curved Composite Sandwich Panels. *Int. J. Mater. Form.* **2020,** *13*: 967-980.
[9] Idczak E. *Topological Optimization of Two-Phase Auxetic Metamaterials*. (in Polish) PhD. thesis, Poznań: Politechnika Poznańska, **2019**.
[10] https://www.simplify3d.com/support/materials-guide/properties-table/?filas=flexible, pla, nylon, [retrevied 09.06.**2021**].
[11] Dobrzański L.A. *Fundamentals of Materials Science and Metallurgy. Engineering Materials with the Basics of Material Design*. (in Polish) Warszawa: Wyd. Naukowo-Techniczne, **2002**.

Received: August 09, 2022
Revised: December 12, 2022
First published online: December 23, 2022